Polymer 50 (2009) 6350–6356

Contents lists available at ScienceDirect

Polymer

journal homepage: www.elsevier.com/locate/polymer

Thermal-induced percolation in high-density polyethylene/carbon black composites

Qing Cao [a], Yihu Song [a,b], Yeqiang Tan [a], Qiang Zheng [a,b,*]

[a] Department of Polymer Science and Engineering, Zhejiang University, Hangzhou 310027, China
[b] Key Laboratory of Macromolecular Synthesis and Functionalization of Ministry of Education, Zhejiang University, Hangzhou 310027, China

ARTICLE INFO

Article history:
Received 23 June 2009
Received in revised form
13 October 2009
Accepted 15 October 2009
Available online 31 October 2009

Keywords:
Annealing
Simultaneous
Percolation

ABSTRACT

The networking of carbon black in high-density polyethylene melt has been traced by simultaneous electrical resistance (R) and dynamic storage modulus (G') testing. Thermal-induced dynamic percolation was observed for both R and G' as a function of annealing time. The influence of temperature and filler volume fraction on percolation times to R and G' was investigated, and activation energies of dynamic percolation were determined. The percolation times were longer than the terminal relaxation time, and activation energies of dynamic percolation were significantly higher than those of viscous flow and molecular relaxation of the composites. A first order kinetics aggregation model was introduced into the classical percolation theory to account for the dynamic percolation. The contribution of filler networking was evaluated quantitatively.

1. Introduction

In carbon black (CB) filled polymers, a conduction network is formed at CB volume fraction (Φ) above percolation threshold (Φ_C) [1] depending on the structure [2] and dispersion [3,4] of CB aggregates as well as the interaction between CB and the matrix [5–7]. The conductive composites are in thermodynamic nonequilibrium so that the formation of conduction network is highly dependent on temperature (T) and time (t) [8–11]. Thermal-treatment at elevated temperatures could accelerate the structural evolution of the percolation network [12,13]. In particular, annealing at temperatures above melting point (T_m) of semi-crystalline matrix causes CB aggregates to agglomerate to form a three-dimensional conduction network, which is accompanied by a drastic change of electrical resistance (R), termed dynamic percolation [14].

Investigating the dynamic percolation is helpful for optimizing annealing conditions to improve positive temperature coefficient (PTC) performance of conductive composites based on semicrystalline polymers [15]. Dynamic light scattering has been utilized to determine the diffusion coefficient of colloidal particles [16–20] in polymer solutions in the dilute regimes. However, it is not applicable to the conductive composites highly filled with CB aggregates. On the other hand, CB has been used as a self-diagnosing probe to trace particle–polymer interaction involved in the relaxation and viscoelasticity of the matrix [21].

Dynamic rheology is sensitive to filler dispersion in polymers [22–26]. The presence of a temporary filler network is responsible for the low-frequency modulus plateau [27,28]. Empirical relationships have been established between dynamic storage modulus (G') measured at $T > T_m$ and electrical resistivity (ρ) measured at room temperature for CB-filled polymers [28–31].

Simultaneous measurement of conductive and rheological properties has been performed in CB-filled natural rubber [32], vulcanizates [33] or electrorheological suspensions [34] under shear actions. We have proposed a novel method for simultaneous measurement of R and G' for conductive polymer composites [35]. By using this method, we have investigated the simultaneous variations of R and G' for CB-filled semicrystalline polymers undergoing shear deformation [36], isothermal crystallization [37] or nonisothermal ramp [38]. In the present article, we focus our attention on the simultaneous measurement of R and G' as a function of t for high-density polyethylene (HDPE)/CB composites subjected to annealing at $T > T_m$. We attempt to clarify the influence of T and Φ on CB networking and the resultant evolution of electrical conduction and dynamic rheological behaviors.

* Corresponding author. Department of Polymer Science and Engineering, Zhejiang University, Hangzhou 310027, China. Fax: +86 571 87952522.
E-mail address: zhengqiang@zju.edu.cn (Q. Zheng).

0032-3861/$ – see front matter © 2009 Elsevier Ltd. All rights reserved.
doi:10.1016/j.polymer.2009.10.059

2. Experimental

2.1. Materials and sample preparation

HDPE (density 0.954 g cm^{-3}, $T_m = 130$ °C, melt flow index 0.09 g min^{-1}) was purchased from Yangzi Petrochem. Corp., China. CB (VX$_c$-605, particle size 25 nm, density 1.85 g cm^{-3}, nitrogen absorption special surface 63 m^2 g^{-1}, and dibutyl phthalate absorption 1480 mm^3 g^{-1}) was obtained from Shanghai Cabot Chem. Co., Ltd., China. Antioxidant (B215, relative molecular mass 647, $T_m = 180$–185 °C) was a product from Ciba–Geigy Co., Japan. HDPE and CB were dried at 70 °C for 30 h before use.

The HDPE/CB composites were prepared by mixing HDPE, CB and antioxidant on a two-roll mill at 160 ± 5 °C and 50 rpm for 10 min. Weight fraction of antioxidant was 2 wt% in the composites. The composites were prepared through compression molded at 160 ± 5 °C and 14.7 MPa for 10 min to form disc samples of 7.9 mm in diameter and 1.2 mm in thickness for simultaneous measurement. Rectangle sheets of 35 mm in length, 10 mm in width and 1.2 mm in thickness were also prepared and two pieces of copper net were mounted onto the opposite wide surfaces of the sheet to ensure good electrical contact with digital multimeter for resistance measurement at room temperature.

2.2. Room-temperature resistance measurement

Room temperature resistance measurement was performed at 25 °C. R of the samples below 1.2 × 10^8 Ω was measured using the two-probe method with an Escort-3146 digital multimeter. R above 1.2 × 10^8 Ω was measured with a high-resistance meter (ZC36, 10^{-14} A and 10^{17} Ω).

2.3. Dynamic rheology and electrical conduction simultaneous measurement

The setup for simultaneous measurement of R and G' was described elsewhere [35]. Rheological measurement was performed on an advanced rheomitric expansion system (ARES, Rheometrics Co., USA) in dynamic time sweep mode under 1% strain with a frequency (ω) of 1 rad s^{-1}. Simultaneously, R was measured with an automatic measurement system where a 7150 plus digital multimeter (Schlumberger) was installed. The applied direct current voltage was 1 V. Experiments with different strain amplitudes showed that the influence of 1% strain on R was negligible [39]. Dynamic frequency sweep was conducted from 10^2 rad s^{-1} to 0.0158 rad s^{-1} under 1–5% strain in the linearity region.

3. Results and discussion

3.1. Percolation at different temperatures

Fig. 1 shows ρ as a function of Φ for the HDPE/CB composites at room temperature. Also shown are the data measured at 160 °C, 180 °C, 200 °C and 220 °C for the composites being annealed at the corresponding temperatures for 3 h. The data at room temperature exhibits the typical percolation transition. ρ drops dramatically by more than 10 orders of magnitude with increasing Φ above $\Phi_C = 0.05$. The curves at elevated temperatures show a similar tendency except for a slight increase in Φ_C to 0.07. At $\Phi < \Phi_C$, ρ at elevated temperatures is over four orders lower than that at room temperature, which might be ascribed to the thermal-excited conduction in the matrix. On the other hand, at $\Phi >> \Phi_C$, ρ at elevated temperatures is higher than that at room temperature, which is attributed to the dilution effect resulting from the matrix melting.

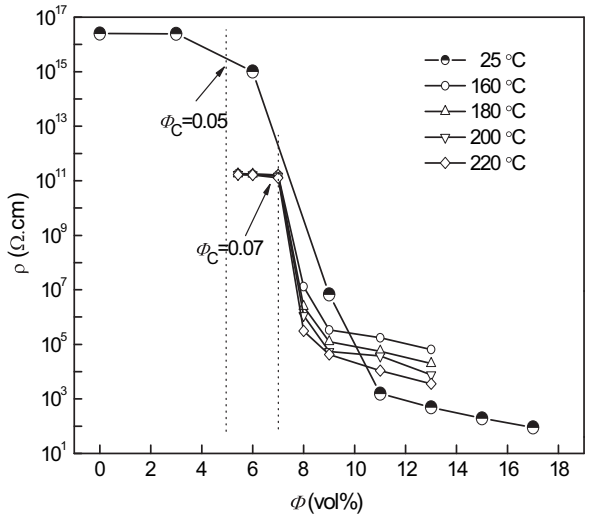

Fig. 1. Volume resistivity (ρ) as a function of CB volume fraction (Φ) for HDPE/CB composites at room temperature and at elevated temperatures after being annealed for 3 h.

3.2. Dynamic percolation

Fig. 2 presents R and G' as a function of t for the composite (Φ = 9 vol%) during annealing at four different temperatures above T_m. At the earlier stage of annealing, R and G' change slightly with t. After critical times denoted as t_{pR} and t_{pG} on the figure, R decreases while G' increases markedly with increasing t, appearing as "dynamic conduction (DC) percolation" and "dynamic modulus (DM) percolation".

Excess interfacial energy of conductive composites is considerably high. CB aggregates in the melt tend to agglomerate in order to reduce excess interfacial energy [5,6], which is accelerated due to annealing at elevated temperatures [40]. The driving force for the agglomeration might be the strong dispersive interaction between CB and the matrix as well as the depletion interaction between adjacent CB aggregates [41]. Wu et al. [21] investigated the DC percolation of CB-filled polymers and ascribed the sharp R decay at $t > t_{pR}$ to the formation of CB network throughout the matrix. In the work of this paper, R and G' were recorded simultaneously during

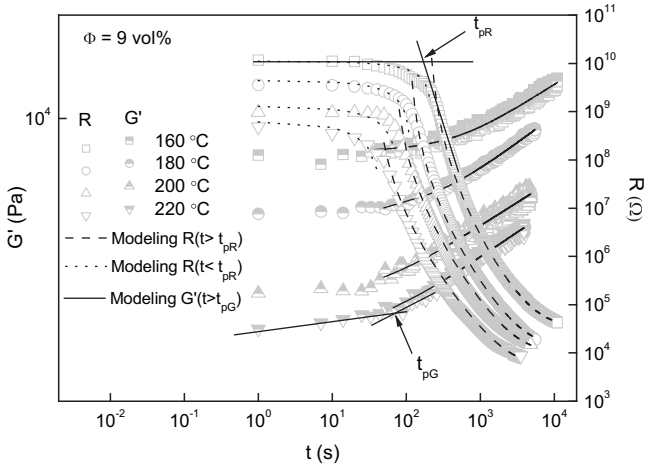

Fig. 2. Storage modulus (G', half-filled symbols) and resistance (R, hollow symbols) as a function of time for the composite with Φ = 9 vol% at four temperatures. The curves are fitted according to the modified percolation model.

annealing. When the composites were heated to a temperature above T_m, the conduction network preexisting in the semi-crystalline state was partially broken down. The R evolution in Fig. 2 thus reflects the reformation of conduction pathways in the melt.

Addition of CB into polymers leads to dramatic changes in viscoelasticity of the melt. The modulus increment due to filling can be mainly ascribed to direct bridging of single chains adsorbed on different aggregates, entanglement between chains adsorbed on separate aggregates, and entanglement of non-adsorbed bulk chains [22,27,42]. Three types of network, a temporary filler network, a temporary polymer network formed by entanglement, and a combined filler-polymer network, have been proposed for explaining the rheological behavior of filled polymers [43]. Incorporation of CB into polymers generally results in a reduction in mobility of polymer chains between CB aggregates [44,45]. At given temperatures, the marked G' increment with t at $t > t_{pG}$ can be ascribed to the gradual formation of the combined network. Similar rheological evolution has been observed in nanotube-filled polymers [46–48]. As shown in Fig. 3, t_{pG} is generally smaller than t_{pR}, suggesting that the combined network responsible for the DM percolation is easier to form in comparison with the CB network responsible for the DC percolation [48].

3.3. Activation energies of dynamic percolation

Fig. 3 gives the critical times t_{pR} and t_{pG} as a function of reciprocal temperature ($1/T$). At given temperatures, both t_{pR} and t_{pG} decrease significantly with increasing Φ. Activation energies of the DC percolation and the DM percolation, ΔE_R and ΔE_G, were determined from the slopes of t_{pR} and t_{pG} against $1/T$ and are shown as a function of Φ in Fig. 4. Both ΔE_R and ΔE_G are nearly independent of Φ at $\Phi = 8$–11 vol%.

It is reported that the aggregation of CB in polymer melts has a close relationship with polymer dynamics [21,49]. To compare the activation energies of dynamic percolation and viscoelasticity, we measured complex viscosity (η^*) as a function of ω for the composites at 160 °C, 180 °C, 200 °C, and 220 °C. Fig. 5a shows master curves of η^* against ω for the HDPE/CB composites at 160 °C. Fig. 5b shows the horizontal and the vertical shift factors, α_η and α_ω, used for constructing the master curves, as a function of $1/T$. η^* increases with increasing Φ due to the reinforcement effect. The Arrhenius plots of α_η and α_ω against $1/T$ in Fig. 5b were used to determine activation energies of viscosity and frequency, ΔE_η and ΔE_ω, and the values are shown in Fig. 4.

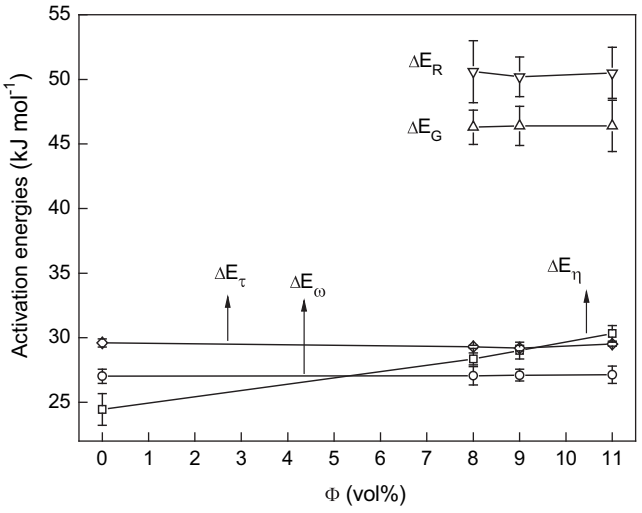

Fig. 4. Activation energies as a function of Φ.

Fig. 6 gives G' and dynamic loss modulus (G'') as a function of ω at 180 °C for pure HDPE and the composites. At a given ω, both G' and G'' increase with increasing Φ due to the reinforcement effect. Both G' and G'' of the composites deviate from the classical linear relationships of $G' \sim \omega^2$ and $G'' \sim \omega$ at $\omega \leq 1$. In particular, G' and G'' of the composite with $\Phi = 11$ vol% appear second plateaus in terminal ω zone, which was ascribed to the formation of three-dimensional CB network throughout the matrix [27,28].

Terminal relaxation time (τ) is an important parameter for evaluating polymer dynamics quantitatively [50]. τ was estimated as the reciprocal of characteristic frequency where G' and G'' intersect with each other as shown in Fig. 6. Fig. 7 shows the Arrhenius plot of τ against $1/T$. At given temperatures, τ increases with increasing Φ, reflecting the reduction of chain mobility due to the restriction of CB particles [44]. The τ value is far smaller than t_{pR} and t_{pG}, indicating that the polymer dynamics may hardly influence the DC percolation and the DM percolation. The activation energy of terminal relaxation time, ΔE_τ, was determined from the slope of τ against $1/T$ and is plotted as a function of Φ in Fig. 4.

As shown in Fig. 4, ΔE_η increases slightly with increasing Φ whereas the others are nearly independent of Φ. In the earlier studies, Wu et al. investigated the DC percolation of CB-filled

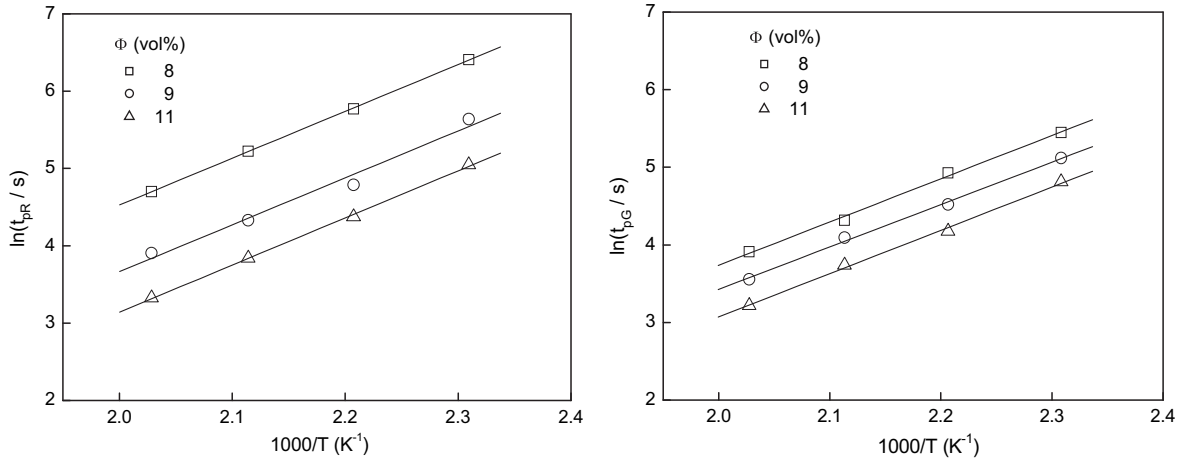

Fig. 3. Arrhenius plots of resistance and modulus percolation times (t_{pR} and t_{pG}) versus reciprocal temperature ($1/T$) for the composites.

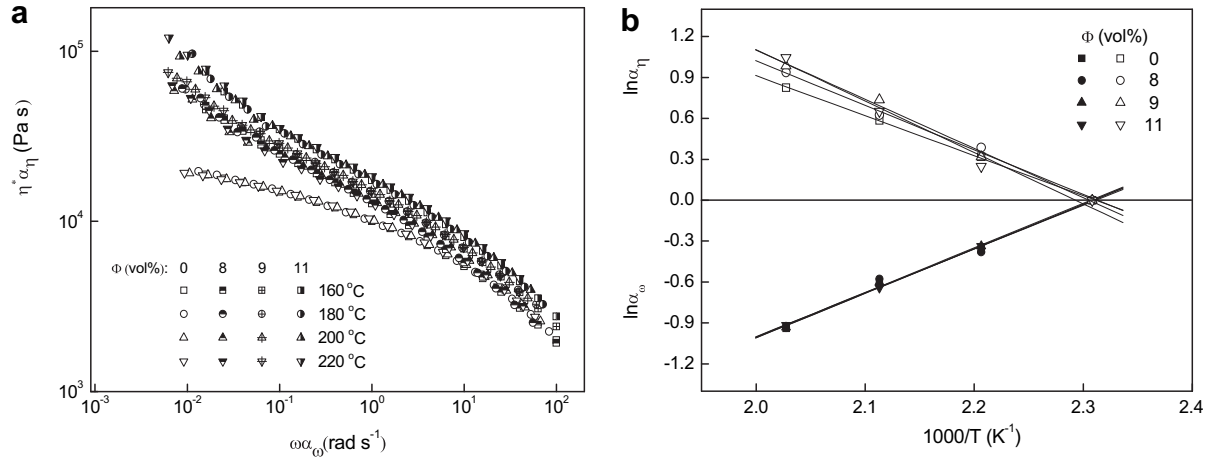

Fig. 5. (a) Master curves of complex viscosity (η^*) as a function of angular frequency (ω) at 160 °C for pure HDPE and for the composites measured at 160 °C, 180 °C, 200 °C, and 220 °C; (b) Arrhenius plot of the horizontal and vertical shift factors (α_η and α_ω) against $1/T$.

polymers and revealed that ΔE_R is closely related to activation energy of zero-shear rate viscosity (η^0) of the matrix [21]. Otherwise, Zhang et al. revealed that ΔE_R approaches activation energy of η^0 of filled polymer composites [49]. As shown in Fig. 4, both ΔE_{pR} and ΔE_{pG} are significantly higher than ΔE_η and ΔE_ω, which are in disagreement with the speculations by Wu and Zhang. The results reveal that the dynamic percolation is more sensitive to temperature in comparison with viscoelasticity of the composites. The difference between ΔE_G and ΔE_R can be understood by taking the two percolation networks into consideration, *i.e.*, the conduction network for charge carrier to transport and the combined network for mechanical momentum to transfer [38]. It is clear that both the DC percolation and the DM percolation are involved in the movement of CB aggregates. The percolation times are much longer than the terminal relaxation time of polymer chains.

3.4. Modeling the DC percolation

Classical percolation theory is well accepted for describing the conduction properties of conductive composites [51,52]. According to this theory, R as a function of Φ can be expressed as

$$R = R_{0F}\left(\frac{\Phi-\Phi_C}{1-\Phi_C}\right)^{-\beta} \quad (\Phi > \Phi_C) \tag{1}$$

$$R = R_{0M}\left(\frac{\Phi_C-\Phi}{\Phi_C}\right)^{s} \quad (\Phi < \Phi_C) \tag{2}$$

Here, β and s are exponents and $\beta = 2$ is usually taken for three-dimensional systems [53–55]. R_{0F} and R_{0M} are constants related to the filler and the matrix, respectively.

The conduction network preexisting at room temperature was partially broken down after the composites were heated to a temperature above T_m. During annealing above T_m, rearrangement of CB aggregates results in the reformation of continuous pathways responsible for the DC percolation. In this case, Φ in Eqs. (1) and (2) should be substituted by a time-dependent effective volume fraction, $\Phi_{eff}(t)$, of interconnected CB aggregates. Φ_C should also be replaced by another parameter Φ_{CR} defined as the minimum CB volume fraction required for the occurrence of DC percolation. Otherwise, the composites with $\Phi < \Phi_{CR}$ do not exhibit DC percolation. Under such treatment, Eqs. (1) and (2) can be modified as

$$R = R_{0F}\left(\frac{\Phi_{eff}(t)-\Phi_{CR}}{1-\Phi_{CR}}\right)^{-\beta} \quad (\Phi > \Phi_C) \tag{3}$$

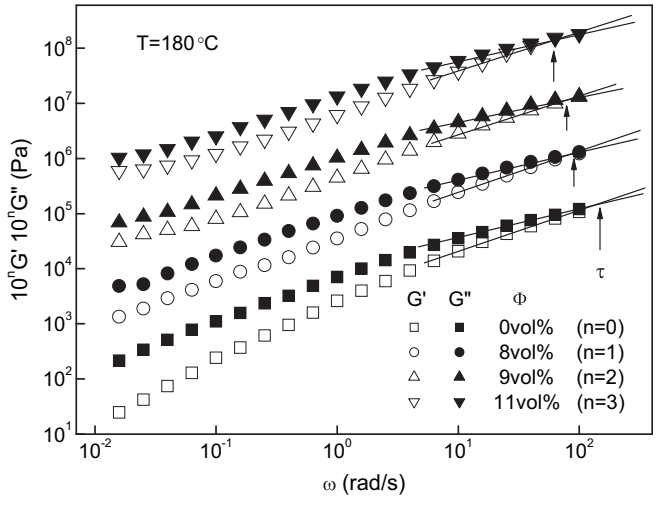

Fig. 6. G' and dynamic loss modulus (G'') as a function of ω at 180 °C for pure HDPE and the composites. The data of G' and G'' are vertically shift by 10^n with the n values indicated.

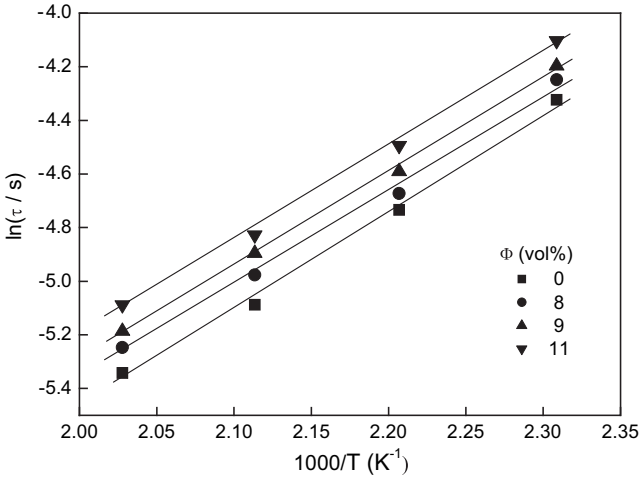

Fig. 7. Relaxation time (τ) as a function of $1/T$ for pure HDPE and the composites.

$$R = R_{0M}\left(\frac{\Phi_{CR} - \Phi_{eff}(t)}{\Phi_{CR}}\right)^{s} (\Phi < \Phi_C) \quad (4)$$

Aggregation of colloidal systems can be described as a cluster–cluster aggregation process. The time-dependences of mean cluster size and its distribution are usually given by solving the Smoluchowski equation [56]. However, the mathematical solution of this equation is often very hard to get. A second order kinetics equation referring to the collision of two particles was proposed for describing the filler networking in composites [57]. The second order kinetics prevails for the particles homogenously distributed in the matrix. However, for the partially broken down network studied here, the CB aggregates are inhomogeneously distributed so that it is hard for the process of "*collision of two particles*" to happen. On the contrary, the networking should follow the first order kinetics governed by the diffusion of isolated small aggregates towards immobilized large aggregates [39]. Neglecting difference in mobilities of aggregates with different sizes, the number of unconnected CB aggregates can reduce under the same kinetic constant K. The Smoluchowski rate equation can be simplified to the first order kinetics [14]

$$\frac{dN(t)}{dt} = KN(t) \quad (5)$$

Integrating Eq. (5) yields

$$\frac{N(t)}{N(\infty)} = 1 - \left[1 - \frac{N(0)}{N(\infty)}\right]\exp(-Kt) \quad (6)$$

or

$$P(t) = 1 - [1 - P(0)]\exp(-Kt) \quad (7)$$

Here, $N(0)$, $N(t)$, and $N(\infty)$ represents the number of interconnected CB particles per unit volume at time zero, t and infinite. $P(0)$ and $P(t)$ represent the fractions of interconnected CB aggregates at time t and infinite.

Assuming that all the CB aggregates are incorporated into the conduction network at time infinite, the time-dependent variable $\Phi_{eff}(t)$ can be expressed as

$$\Phi_{eff}(t) = P(t)\Phi \quad (8)$$

In the DC percolation, continuous CB pathways begin to form only after t_{pR}. Then, the fraction of interconnected CB aggregates reaches Φ_{CR} at t_{pR},

$$\Phi_{eff}(t_{pR}) = \Phi_{CR} = \Phi P(t_{pR}) = \Phi\{1 - [1 - P(0)]\exp(-Kt_{pR})\} \quad (9)$$

Substituting Eqs. (7), (8) and (9) into Eqs. (3) and (4) yields

$$R = A\left[\exp(-Kt_{pR}) - \exp(-Kt)\right]^{-\beta} (t > t_{pR}) \quad (10)$$

$$R = B\left[\exp(-Kt) - \exp(-Kt_{pR})\right]^{s} (t < t_{pR}) \quad (11)$$

Here, $A = R_{0F}\left\{\frac{\Phi[1-P(0)]}{1-\Phi_{CR}}\right\}^{-\beta}$ and $B = R_{0M}\left\{\frac{\Phi[1-P(0)]}{\Phi_{CR}}\right\}^{s}$ are constants depending on Φ and T.

Fig. 8 presents Φ against $1/t_{pR}$ at different annealing temperatures. Φ_{CR} is determined as 0.07 by linearly extrapolating $1/t_{pR}$ to zero [49]. Φ_{CR} is irrespective of T and is the same as the percolation threshold at $T > T_m$, as shown in Fig. 1. Eqs. (10) and (11) are used to fit the experimental data of R against t above and below t_{pR}, respectively. The best fitting results are shown as dashed and dotted curves in Fig. 2. Table 1 lists the parameter values averaged

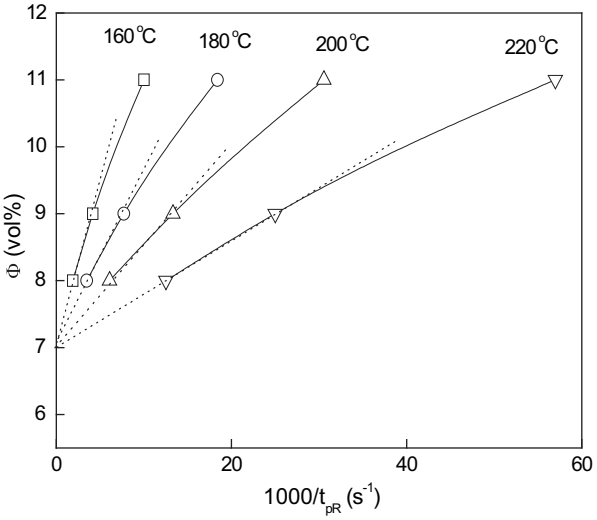

Fig. 8. Relationship between t_{pR} and Φ at different annealing temperatures.

from at least three independent experiments. With the K, t_{pR} and Φ_{CR} values obtained, the value of 1-$P(0)$ was calculated according to Eq. (9) and the results are listed in Table 1.

As shown in Table 1, K increases with increasing T but it is insensitive to Φ, indicating that the movement of isolated CB aggregates is a diffusion-limited process [58]. Fig. 9 shows the relationship between K and $1/\eta^0$ of HDPE. Here, η^0 is taken as the ω-independent η^* plateau value in the terminal region in Fig. 5a. K is linearly dependent on $1/\eta^0$, revealing that the diffusion of CB aggregates is closely related to the viscosity of the matrix. The parameters A and B decrease with increasing T and Φ. The K values ($2.0–7.0 \times 10^{-4}\ s^{-1}$) are considerably small so that A approximates R at time infinite according to Eq. (10). The value of β decreases with increasing T and Φ, showing the tendency to approach the universal value of 2. A variation of β value depending on CB grade as well as the type and microstructure of matrix has been observed in CB-filled rubbers at room temperature, which is ascribed to the kinetic aggregation of CB particles and the resultant alteration of the local structure of the percolation network [52]. The value of s is usually taken as 0.73 in classical percolation [59,60]. However, s is not a constant in the DC percolation, approaching to 0.73 with decreasing T.

The value of 1-$P(0)$ decreases slightly with increasing T. $P(0)$ is about 0.86, 0.77 and 0.62 for the composites with $\Phi = 8$ vol%, 9 vol% and 11 vol%, suggesting that most CB aggregates are interconnected at the beginning of annealing. $P(0)$ increases slightly with increasing T, resulting in a reduction of R with T at earlier stage of

Table 1
Fitting parameters for the modified percolation model.

Φ (vol%)	T (°C)	K (10^{-4} s^{-1})	A (kΩ)	B (10^{10} Ω)	β	s	1-P(0)	K_1 (10^{-5} s^{-1})	α
8	160	2.3	1500	11.0	3.40	0.78	0.143	2.3	0.10
	180	3.2	700	9.7	2.92	0.82	0.141	2.5	0.13
	200	4.5	300	9.1	2.75	0.85	0.138	2.3	0.15
	220	6.4	120	8.5	2.51	0.91	0.132	3.1	0.13
9	160	2.5	31	9.8	2.65	0.76	0.235	2.0	0.14
	180	3.3	12	6.9	2.52	0.85	0.231	2. 7	0.17
	200	4.7	9.5	3.8	2.40	0.94	0.230	2.6	0.18
	220	6.3	6.5	2.5	2.22	1.06	0.228	2.5	0.15
11	160	2.5	20	8.2	2.51	0.74	0.375	2.4	0.15
	180	3.3	8.2	5.3	2.42	0.87	0.372	2.6	0.16
	200	4.6	6.5	2.7	2.35	1.07	0.367	2.6	0.16
	220	6.5	5.6	1.2	2.10	1.21	0.369	2.6	0.18

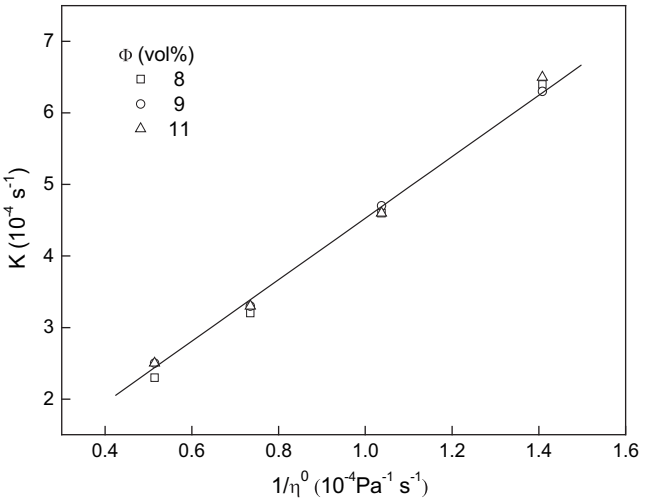

Fig. 9. Kinetic constant (K) of the composites as a function of reciprocal zero-shear rate viscosity ($1/\eta^0$) of the pure HDPE.

annealing as shown in Fig. 2. The variation of $P(0)$ with respect to T could account for the negative temperature coefficient (NTC) effect of resistance usually observed in HDPE/CB composites above T_m. Upon heating the composites across T_m from below, the large volume expansion resulting from the matrix melting destroys the preexisting conduction network, leading to the partial breakdown of conduction network accompanied with the PTC effect. The DC percolation during annealing is not involved in all the aggregates with a wide distribution of size. Most likely, the diffusion of isolated small aggregates in the melt gradually interconnects the adjacent clusters, which rebuilds the conduction network upon annealing.

3.5. Modeling the DM percolation

As shown in Fig. 2, annealing causes G' to increase less than one order of magnitude at $t \leq 10^4$ s. The variation amplitude is much smaller than the R decay at the same time scale. The difference in variation magnitudes of R and G' can be explained on the basis of different mechanisms. The former is related to the close CB electrical contact for charge carrier to transport, while the later is related to the viscous coupling between CB particles and polymer chains for mechanical momentum to transfer [39]. Being different from the DC percolation, polymer chains must participate in the DM percolation. There is no doubt that the chain bridging, together with the direct CB contact, plays an important role in the DM percolation.

G' of filled polymers is usually expressed as a power law [48]

$$G' \sim (\Phi - \Phi_{CG})^{\alpha} (\Phi > \Phi_{CG}) \tag{12}$$

where Φ_{CG} is a threshold of modulus and α is a critical exponent. In the DM percolation, Φ should be replaced by $\Phi_{eff}(t)$,

$$G(t) \sim [P(t)\Phi - \Phi_{CG}]^{\alpha} (\Phi > \Phi_{CG}) \tag{13}$$

Being similar to the DC percolation, Eq. (13) can be modified to

$$G'(t) \sim [\Phi(1 - P(0))]^{\alpha} [\exp(-K_1 t_{pG}) - \exp(-K_1 t)]^{\alpha} (t > t_{pG}) \tag{14}$$

The kinetics parameter K_1 differs from K because of the different mechanisms in the DM percolation and the DC percolation. Eq. (14) was applied to fit G' as a function of t using the least-square method and the fitting results are shown as solid curves in Fig. 2. The values of K_1 and α averaged from at least three independent experiments are listed in Table 1. Both K_1 and α seem independent of T and Φ and their average values are $K_1 = (2.5 \pm 0.3) \times 10^{-5}$ s^{-1} and $\alpha = 0.15 \pm 0.02$. The fitting results suggest that the DM percolation follows a universal law. The value of K_1 is about one order of magnitude smaller than K, which is in agreement with the observation that the DM percolation is much slower than the DC percolation.

4. Conclusions

Thermal-induced DC percolation and DM percolation take place simultaneously during annealing HDPE/CB composites at $T > T_m$. The percolation times, t_{pR} and t_{pG}, are much longer than the terminal relaxation time of the composites. The activation energies, ΔE_{pR} and ΔE_{pG}, are much higher than those of viscous flow of the composites and of the terminal relaxation time of the matrix.

The first order kinetic particle aggregation model is introduced into the classical percolation theory to describe the DC percolation. The reformation of CB network, which has been partially broken down due to melting of the matrix, can well account for the DC percolation. Similar treatment is applicable to the DM percolation. The kinetics parameter K_1 in the DM percolation is about one order of magnitude smaller than K in the DC percolation. The critical exponents β and s in the DC percolation are strongly dependent on T and Φ. On the other hand, the critical exponent α in the DM percolation seems to be a constant.

Acknowledgement

This work was supported by the National Natural Science Foundation of China (No. 20774085).

References

[1] Medalia AI. Rubber Chem Technol 1985;59(3):432–54.
[2] Janzen J. J Appl Phys 1975;46(2):966–9.
[3] Garncarek Z, Piaseck R, Boreck J, Maj A, Sudol M. J Phys D Appl Phys 1996;29(5):1360–6.
[4] Gubbels F, Blacher S, Vanlathem E, Jerome R, Deltour R, Brouers F, et al. Macromolecules 1995;28(5):1559–66.
[5] Miyasaka K, Watanabe K, Jojima E, Aida H, Sumita M, Ishikawa K. J Mater Sci 1982;17(6):1610–6.
[6] Sumita M, Asai S, Miyadera N, Jojima E, Miyasaka K. Colloid Polym Sci 1986;264(3):212–7.
[7] Mamunya EP, Davidenko VV, Lebedev EV. Compos Interfaces 1997;4(4):169–76.
[8] Zhang C, Wang P, Ma CA, Wu GZ, Sumita M. Polymer 2006;47(1):466–73.
[9] Katada A, Konishi Y, Isogai T, Tominaga Y, Asai S, Sumita M. J Appl Polym Sci 2003;89(4):1151–5.
[10] Traina M, Pegoretti A, Penati A. J Appl Polym Sci 2007;106(3):2065–74.
[11] Yi XS. Function principle of filled conductive polymer composites. Beijing: National Defense Industry Press; 2004 [chapter 4].
[12] Böhm GGA, Nguyen MN. J Appl Polym Sci 1995;55(7):1041–50.
[13] Cipriano BH, Kota AK, Gershon AL, Laskowski CJ, Kashiwagi T, Bruck HA, et al. Polymer 2008;49(22):4846–51.
[14] Wu GZ, Asai S, Zhang C, Miura T, Sumita M. J Appl Phys 2000;88(3):1480–7.
[15] Song YH, Zheng Q. J Appl Polym Sci 2007;105(2):710–7.
[16] Won J, Onyenemezu C, Miller WG, Lodge TP. Macromolecules 1994;27(25):7389–96.
[17] Dunstan DE, Stokes J. Macromolecules 2000;33(1):193–8.
[18] Lehner D, Lindner H, Glatter O. Langmuir 2000;16(4):1689–95.
[19] Brauce BJ, Robert DP. Dynamic light scattering. New York: Wiley; 1976 [chapter 2].
[20] Bezot P, Hesse-Bezot C. Kinetics of clustering of carbon black suspensions by light scattering techniques. Physica A 1999;271(1):9–22.
[21] Wu GZ, Asai S, Sumita M. Macromolecules 2002;35(5):1708–13.
[22] Bar-Chaput S, Carrot C. Rheologica Acta 2006;45(4):339–47.
[23] Konishi Y, Cakmak M. Polymer 2006;47(15):5371–91.
[24] Cassagnau Ph. Polymer 2008;49(9):2183–96.
[25] Wu G, Lin J, Zheng Q, Zhang MQ. Polymer 2006;37(7):2442–7.
[26] Das A, Stöckelhuber KW, Jurk R, Saphiannikova M, Fritzsche J, Lorenz H, et al. Polymer 2008;49(24):5276–83.
[27] Aranguren MI, Mora E, DeGroot JJ, Macosko CW. J Rheol 1992;36(6):1165–82.

[28] Wu G, Zheng Q. J Polym Sci Part B Polym Phys 2004;42(7):1199–205.
[29] Wu GZ, Asai S, Sumita M, Hattori T, Higuchi R, Washiyama J. Collid Polym Sci 2000;278(3):220–8.
[30] Zheng Q, Song YH, Wu G, Song XB. J Polym Sci Part B Polym Phys 2003;41(9): 983–92.
[31] Kotsikova R, Nesheva D, Krusteva E, Stavrev S. J Appl Polym Sci 2004;92(4): 2220–7.
[32] Payne AR. J Appl Polym Sci 1965;9(3):1073–182.
[33] Voet A, Cook FR. Rubber Chem Technol 1968;41(5):1207–14.
[34] Pan XD, Mckinley GH. Langmuir 1998;14(5):985–9.
[35] Liu ZH, Song YH, Zhou JF, Zheng Q. J Mater Sci 2007;42(20):8757–9.
[36] Liu ZH, Song YH, Shangguan YG, Zheng Q. J Mater Sci 2007;42(8):2903–6.
[37] Liu ZH, Song YH, Shangguan YG, Zheng Q. J Mater Sci 2008;43(14):4828–33.
[38] Zhou JF, Song YH, Shangguan YG, Zheng Q. J Appl Polym Sci 2008;110(4): 2001–8.
[39] Alig I, Skipa T, Lellinger D, Potschke P. Polymer 2008;49(16):3524–32.
[40] Grossiord N, Kivit PJJ, Loos J, Meuldijk J, Kyrylyuk AV, Schoot PVD, et al. Polymer 2008;49(12):2866–72.
[41] Meier JG, Mani JW, Klüppel M. Phys Rev B 2007;75(5):054202.
[42] Cassagnau Ph, Melis F. Polymer 2003;44(21):6607–15.
[43] Pötschke P, Abel-Goad M, Alig I, Dudkin S, Lellinger D. Polymer 2004;45(26):8863–70.
[44] Lipatov Yu. Adv Polym Sci 1977;22:1–59.
[45] Karasek L, Sumita M. J Mater Sci 1996;31(2):281–9.
[46] Pötschke P, Fornes TD, Paul DR. Polymer 2002;43(11):3247–55.
[47] Meincke O, Kaempfer D, Weickmann W, Friedrich C, Vathauer M, Warth H. Polymer 2004;45(3):739–48.
[48] Du F, Scogna RC, Zhou W, Brand S, Fischer JE, Winey KI. Macromolecules 2004;37(24):9048–55.
[49] Zhang C, Wang L, Wang JL, Ma CA. Carbon 2008;46(15):2053–8.
[50] Ferry JD. Viscoelastic properties of polymer. 3rd ed. New York: John Wiley & Sons; 1980 [chapter 2].
[51] Pötschke P, Dudkin SM, Alig I. Polymer 2003;44(17):5023–30.
[52] Klüppel M. Adv Polym Sci 2003;164(1):1–86.
[53] Bunde A, Havlin S. Fractals and disordered systems. Berlin, Heidelberg: Springer-Verlag; 1991 [chapter 2].
[54] Adler J, Meir Y, Aharony A, Harris AB, Klein L. J Stat Phys 1990;58(3):511–38.
[55] Gingold DB, Lobb CJ. Phys Rev B 1990;42(13):8220–4.
[56] Jullien R, Botet R. Aggregation and fractal aggregates. Singapore: World Scientific; 1987 [chapter 2].
[57] Alig I, Skipa T, Lellinger D, Pegel S, Pötschke P. Phys Status Solidi B 2007; 244(11):4223–6.
[58] Allen PEM, Patrick CR. Kinetics and mechanisms of polymerization reaction-application of physico–chemical principles. New York: Wiley; 1974 [chapter 2].
[59] Stauffer D, Aharony A. Introduction to percolation theory. 2nd ed. London: Taylor & Francis; 1992 [chapter 3].
[60] Herrmann HJ, Derrida B, Vannimenus J. Phys Rev B 1984;30(7):4080–2.